

LEP Summer Study/1-6
October, 1978

LEP SUMMER STUDY

Organized under the Joint Sponsorship of

ECFA and CERN

Les Houches and CERN

10 to 22 September, 1978

POLARIZATION AT LEP ENERGIES

by

P. Darriulat, CERN

Copies available upon request from Ch. Redman, CERN/ISR
LEP Summer Study Secretariat

1. Introduction

Polarization at LEP was not the subject of specific studies in a specialized working group at Les Houches, but its various aspects have been examined in each of the working groups separately¹⁾. Reviews were presented on several occasions, both of the implications it has on the machine front²⁾ and of the possibilities it offers for physics³⁾. The present note is an attempt at giving a brief and elementary summary of the present ideas in this domain.

Beam polarization is expected to induce spectacular effects at LEP. This contrasts with proton (or antiproton) machines which we use as parton (quarks and gluons) accelerators, and where the incident polarization in a parton-parton collision is not simply related to that of the composite incident protons. The situation is completely different in e^+e^- annihilation processes, where the quantum numbers of the intermediate state are precisely those of the incident beams. In addition, electromagnetic and weak interactions, for which LEP is a privileged laboratory, proceed via couplings which induce effects having characteristic dependences upon the incident electron helicities. As an example, at the Z^0 pole, the interaction rate is expected to increase by three orders of magnitude when switching from $e_L^- e_L^+$ to $e_L^- e_R^+$! The mere possibility of such a dramatic effect is sufficient proof of the potential power of a polarized beam facility for experimentation at LEP.

However, technical difficulties attached to its implementation, constraints it imposes on the machine design, and limitations in its expected performance invite us to make a more careful evaluation of the advantages it would provide for physics.

2. Polarizing the Beams

The present section gives a very elementary and superficial presentation of the basic principles. In addition to original articles^{2,4,5)}; excellent reviews²⁾ are available on this topic.

2.1 Spin Motion

The motion of a spinning electron circulating in the machine is governed by

$$\frac{d\vec{\sigma}}{dt} = \vec{\sigma} \times \vec{\Omega} + \text{spin-flip terms} \quad (1)$$

where $\vec{\sigma}$ is the electron spin (more precisely its mean value calculated from the density matrix describing the beam) expressed in the local frame rotating with the electron (Fig. 1). The rotation frequency of the particle on its orbit (radius R) is $\omega_0 = \frac{c}{R} \approx 85$ kHz, independent of the energy E.

The vector $\vec{\Omega}$ around which the spin precesses has its major component Ω_{\perp} directed along the guide field. Electric fields can usually be neglected. The precession frequency Ω_{\perp} increases with energy

$$\Omega_{\perp} = \omega_0 E \frac{\alpha}{2\pi m} = \omega_0 \frac{E}{440 \text{ MeV}} \quad (2)$$

Here α is the fine-structure constant; $\frac{\alpha}{2\pi} = \frac{g-2}{2}$; g is the gyromagnetic ratio of the electron and m its rest mass. At $E = 70 \text{ GeV}$ the spin precesses about 160 times per revolution.

Magnetic fields directed along the particle velocity contribute to Ω_{\parallel} but in a high energy machine their effect is small: at $E = 70 \text{ GeV}$, a complete turn of the spin vector around the particle velocity requires a field strength of $\approx 14680 \text{ kGm}$. Field inhomogeneities induce small radial and longitudinal components of $\vec{\Omega}$ which result in oscillations of σ_{\perp} , the spin component parallel to the guide field (Fig. 2). As long as these oscillations remain small enough, their net effect is simply to slightly reduce the transverse polarization. In high energy machines radial field inhomogeneities are the dominant source of such oscillations.

2.2 Transverse Polarization⁴⁾

The "spin-flip" terms in Eq. 1 correspond to spin-flip emission of synchrotron radiation, which occurs with a probability per unit time

$$\Omega_{\text{sf}} = \frac{5\sqrt{3}}{16\alpha} \left(\frac{r}{R}\right)^2 \gamma^5 \omega_0 F(\vec{\sigma}) \quad (3)$$

where $F(\vec{\sigma}) = 1 - \frac{2}{9} \sigma_{\parallel}^2 + \frac{8\sqrt{3}}{15} \sigma_{\perp}$ (4)

Here, r is the electron radius, $\approx 2.8 \text{ fm}$, and $\gamma = E/m$. Owing to the linear dependence of F upon σ_{\perp} , a transverse polarization P , directed along the guide field (for e^+ , or against it for e^-) builds up with a characteristic time (Fig. 3)

$$T = \frac{F(\vec{\sigma})}{\Omega_{\text{sf}}} \approx \left(\frac{E}{70}\right)^{-5} \times 20 \text{ minutes} \quad (5)$$

At equilibrium the polarization reaches a value P_{max} such that

$$\frac{1 - P_{\text{max}}}{2} \left(1 + \frac{8\sqrt{3}}{15}\right) = \frac{1 + P_{\text{max}}}{2} \left(1 - \frac{8\sqrt{3}}{15}\right)$$

$$P_{\text{max}} = \frac{8\sqrt{3}}{15} \approx 0.924 \quad (6)$$

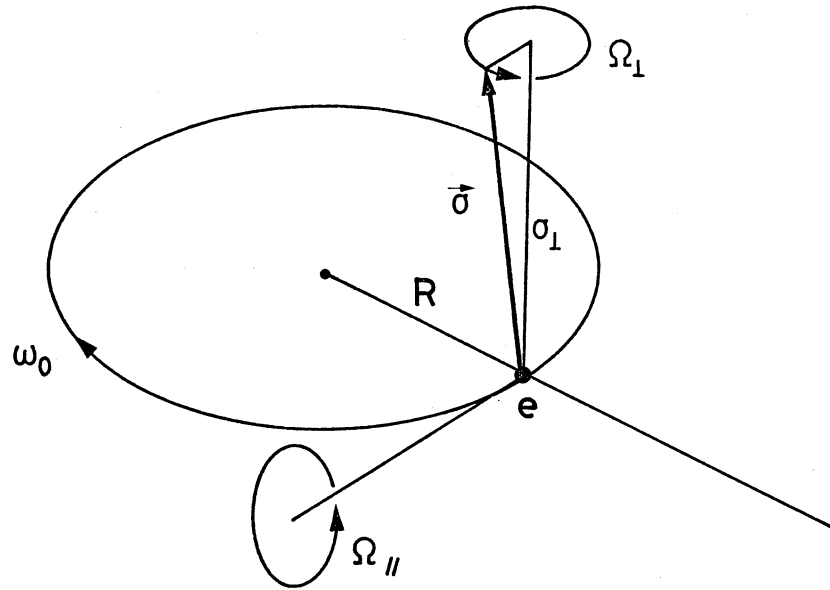


Figure 1 : Variables describing the spin motion

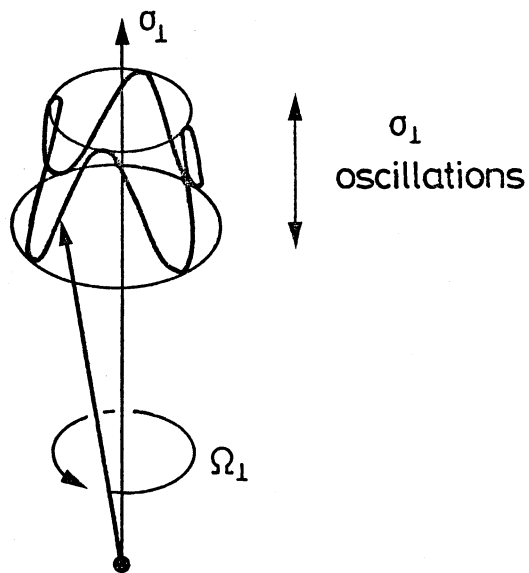


Figure 2 : Spin oscillations and precession

The fraction f of synchrotron radiation power is usually very small, of the order of $1.26 \cdot 10^{-11}$ at $E = 70$ GeV:

$$f \approx \frac{3}{\alpha^2} \left(\frac{r}{R} \right)^2 \gamma^4$$

The critical energy where f is of order unity is of the order of 40 TeV corresponding to $\gamma_c = \left(\frac{\alpha}{\sqrt{3}} \frac{R}{r} \right)^{\frac{1}{2}}$. The spin-flip terms are responsible for a spontaneous build-up of transverse polarization, which however will only become sizable at high energies ($T \approx 20$ minutes at $E = 70$ GeV, ≈ 2 hours at $E = 50$ GeV).

2.3 Depolarizing Resonances

In the above discussion it was implicitly assumed that field inhomogeneities drive only small oscillations of σ_{\perp} around its mean value; this is unfortunately not the case at LEP where depolarizing resonances preclude the successful completion of the polarization process.

Spin resonances are very similar to more familiar resonances such as those occurring in betatron and synchrotron oscillations; it may therefore be useful to review briefly the mechanism of betatron resonances before considering the spin case.

Possible trajectories in a given machine are defined from their deviations from the closed orbit; transverse deviations correspond to betatron oscillations, longitudinal (energy) deviations to synchrotron oscillations. The radial deviation $x(s)$, where s is the azimuthal coordinate along the machine, can be written

$$\left. \begin{aligned} x(s) &= a\sqrt{\beta(s)} \cos(\phi(s) - \theta) \\ \phi(s) &= \int_0^s \frac{ds'}{\beta(s')} \end{aligned} \right\} \quad (7)$$

Eqs (7) define a two-parameter (a and θ) family of possible trajectories (Fig. 4). At fixed s , x takes values ranging between $-a\sqrt{\beta(s)}$ and $+a\sqrt{\beta(s)}$ depending on the phase advance per turn (Fig. 5)

$$\phi(L) - \phi(0) = \oint \frac{ds'}{\beta(s')} = 2\pi Q_x$$

where $L = \oint ds' \approx 2\pi R$.

When a small perturbation is introduced at $s = 0$, such as a transverse kick causing a jump δ of $x' = \frac{dx}{ds}$, the new family of possible trajectories is centred around a new (disturbed) closed orbit defined by its deviation $\Delta x(s)$ from the original one. Everywhere but at $s = 0$, $\Delta x(s)$ satisfies Eq. (7); at $s = 0$

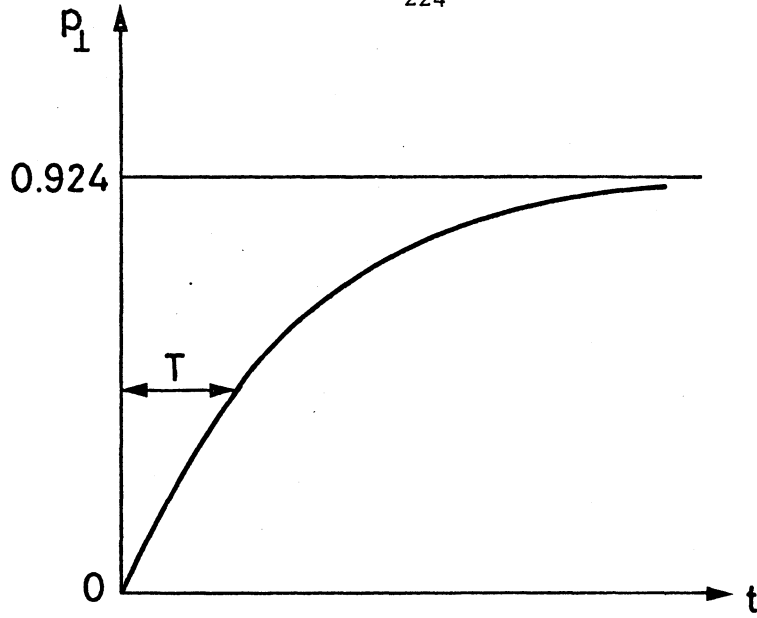


Figure 3 : Spontaneous build-up of transverse polarization P_{\perp} as a function of time t

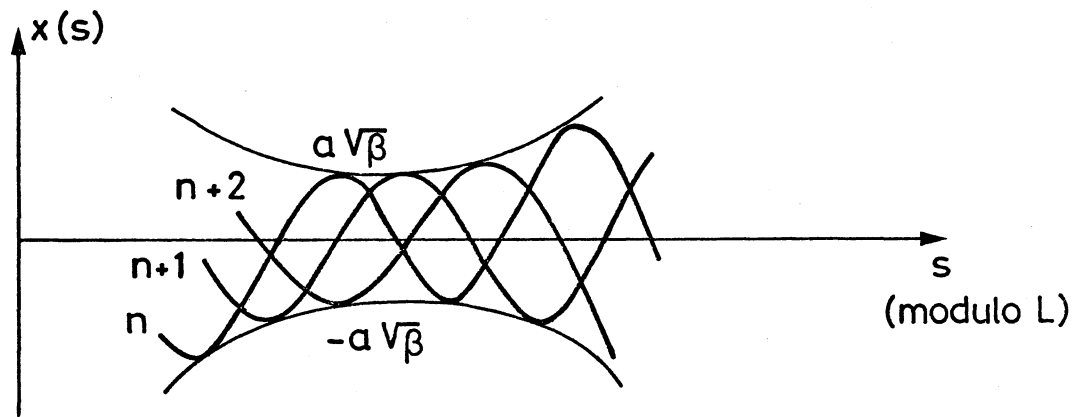


Figure 4 : Betatron oscillations: an electron trajectory at the n -th, $n + 1$ -th and $n + 2$ -th turns. The envelopes $x(s) = \pm a\sqrt{\beta(s)}$ are indicated

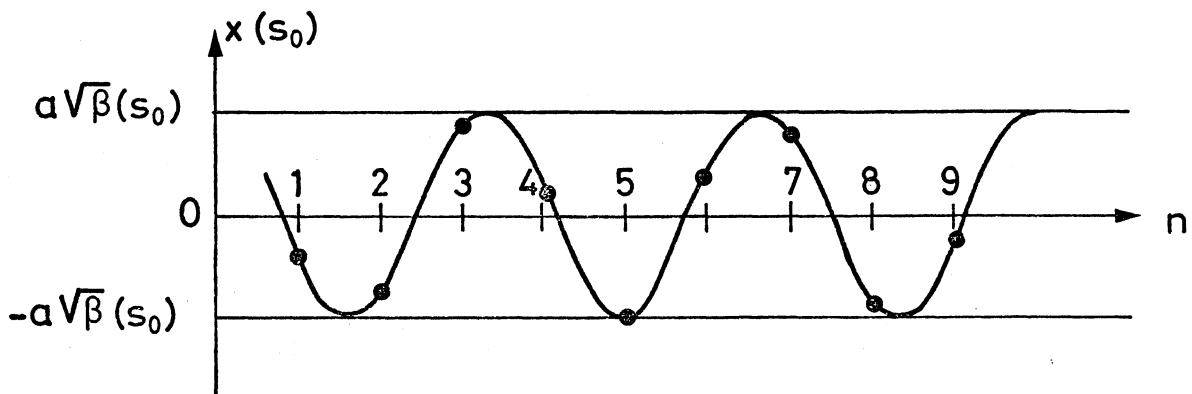


Figure 5 : Deviations of an electron at $s = s_0$ for successive passages

the continuity of the new closed orbit implies

$$\left. \begin{aligned} \Delta x(L) &= \Delta x(0) \\ \Delta x'(L) &= \Delta x'(0) + \delta \end{aligned} \right\} \quad (9)$$

Solving in a and θ we obtain

$$\left. \begin{aligned} \theta &= \pi Q_x \\ a &= \frac{\delta \sqrt{\beta(s)}}{2 \sin \pi Q_x} \end{aligned} \right\} \quad (10)$$

If Q_x takes integer values, a becomes infinite: there is no closed orbit in the perturbed machine; it corresponds to a resonance condition for which no beam can be kept (Fig. 6).

The same applies for vertical betatron oscillations (Q_y) and for synchrotron oscillations (Q_s), the general resonance condition being satisfied whenever

$$n_x Q_x + n_y Q_y + n_s Q_s = \text{integer}, \quad (11)$$

where the three n 's are integer numbers and where the Q 's take the following values at LEP:

$$\begin{aligned} Q_x &= 66.208 \\ Q_y &= 74.272 \\ Q_s &= 0.1075. \end{aligned}$$

In the spin case the closed-orbit equivalent is obtained when the spin is directed along the guide field; the spin-precession around the guide field corresponds to $\phi(s)$, with a phase advance per turn

$$Q_{\uparrow} = \frac{\alpha E}{2\pi m} = \frac{E}{440 \text{ MeV}} \quad (12)$$

As in the case of betatron oscillations, a small perturbation will cause a divergent increase of the amplitude of the σ_{\perp} oscillations, and therefore will destroy polarization, whenever

$$Q_{\uparrow} = n_0 + n_x Q_x + n_y Q_y + n_s Q_s. \quad (13)$$

A set of Q values which satisfies Eq. 13 corresponds to a depolarizing resonance. In particular, for two neighbour resonances corresponding to n_0 and $n_0 + 1$, we have

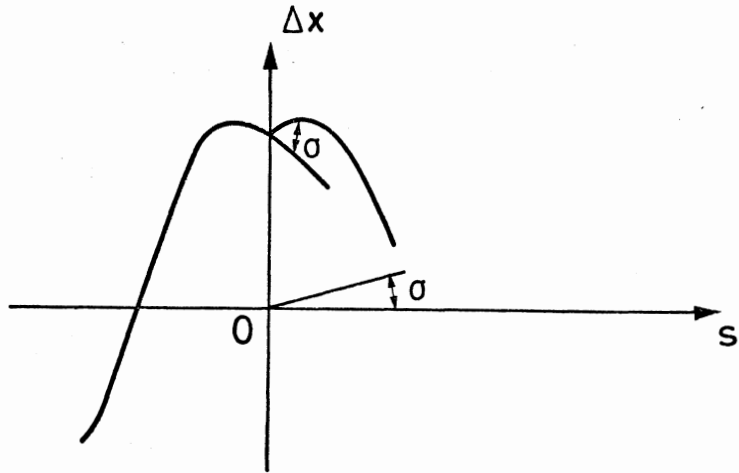
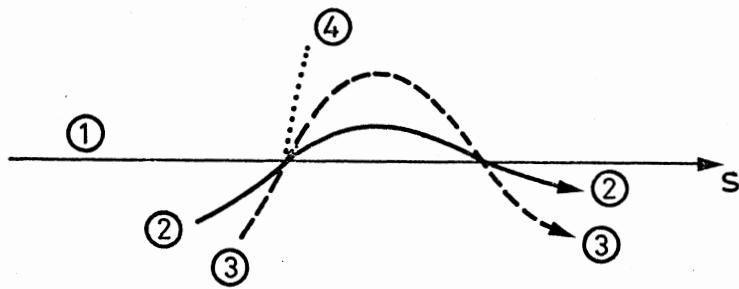


Figure 6 : a) Disturbed closed orbit for a perturbation $\delta = x'(L) - x'(0)$ at $s = 0$



b) Resonant case: the electron trajectory as seen in successive passages

$$\Delta Q_{\uparrow} = 1, \Delta E = 440 \text{ MeV} \quad (14)$$

The beam energy spread at $E = 70 \text{ GeV}$ is approximately Gaussian with variance $\sigma_E \approx 86 \text{ MeV}$, a value as large as one fifth of the energy spacing between neighbour depolarizing resonances: this is sufficient²⁾ to cause a rapid depolarization. As a result, spontaneous transverse polarization has no time to build up at LEP.

2.4 The Siberian Snake Scheme⁵⁾

Depolarizing resonances would in principle be avoided if Q_{\uparrow} could be made energy independent. A typical example of a configuration where this is achieved is provided by 8-shaped machines (Fig. 7). In such machines the precession accumulated in one loop of the 8 is exactly compensated in the other loop with a net result, independent of energy, $Q_{\uparrow} = 0$. Any spin configuration corresponds to a closed solution.

A similar situation is obtained with the Siberian Snake scheme^{2,5)} which can be implemented in a circular machine. It consists of introducing a 180° spin rotation around the beam at some fixed location (S) in the machine. There exist two closed solutions, with the spin parallel or anti-parallel to the electron velocity at S' diametrically opposite to S (Fig. 8). Transverse spin components change sign after one turn, corresponding to $Q_{\uparrow} = \frac{1}{2}$, an energy-independent value, far from integers. Longitudinal polarization can therefore be maintained without suffering from depolarizing resonances.

This very elegant scheme is proposed as an option for LEP but its actual implementation has several important consequences:

- (i) A storage ring injector with a short spontaneous polarization time is necessary. Injection lines allowing for spin rotation to left or right helicity states have to be provided for each beam separately.
- (ii) It does not seem feasible in practice to use a solenoid to drive the 180° spin rotation: 7330 kGm would be necessary at $E = 70 \text{ GeV}$! A set of horizontal and vertical bending magnets (the snake) rotates the spin with a much smaller field strength but alters the orbit as well: for a fixed snake geometry the polarization is optimized at a single energy (which may be modified during shutdowns) and depressed otherwise. The present LEP design requires one of the eight interaction regions to be devoted to the snake.
- (iii) Polarization is optimized in the interaction directly opposite to the snake but is usually depressed elsewhere.

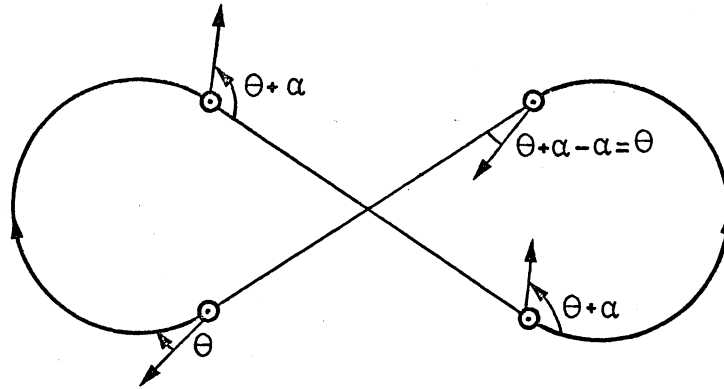


Figure 7 : Spin motion in an 8-shaped machine

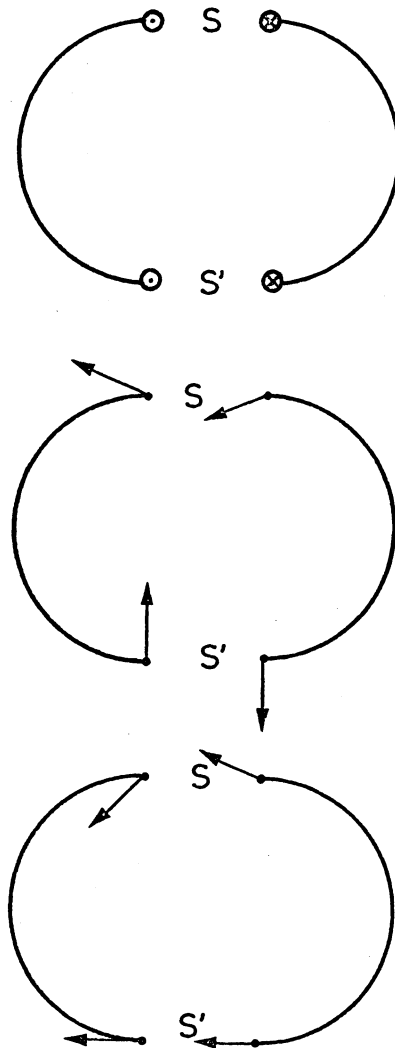


Figure 8 : Siberian Snake Scheme: the snake inserted at s induces an 180° spin precession around the electron velocity

- (iv) Spin-flip emission of synchrotron radiation induces depolarization with a characteristic time⁷⁾ $T \approx (70/E)^5 \times 20$ minutes.
- (v) Introducing the snake breaks the machine periodicity, which may have unpleasant consequences on beam optics.

2.5 Summary

There seems to exist a possible scheme to maintain longitudinal polarization in the machine. However sizable polarizations would not be obtained at all energies (and in particular seem excluded above 70 GeV) nor at all interaction points. The maximum polarization which can be obtained is in principle 92.4% but substantially lower values should be expected in practice.

Detailed studies should be actively pursued to answer the following questions:

- how much depolarization is expected from other sources (experimental magnets, ...),
- how much does the snake disturb beam optics,
- are there alternatives to the Siberian Snake scheme^{8,9)}.

The study of polarization effects at PETRA and PEP will be very informative for the injector design. Recent measurements performed at SPEAR by a SLAC-Wisconsin Collaboration were reported at Les Houches by R. Schwitters¹⁰⁾. The excellent quality of the data produced (Figs. 9 to 11) is very encouraging.

3. Physics Considerations

As we see it today, physics at LEP may schematically be split into two main regions of interest:

- one located in the vicinity of the Z^0 pole where the various Z^0 couplings will be measured; the enhanced cross-section at the pole will permit the study of low branching ratio decay modes. This region is well covered by the machine version using conventional RF cavities. Our present knowledge of weak neutral currents in other sectors is such that important effects are expected in this region: their absence would set dramatic constraints on any theory;
- the other region demands high energies and is covered by the machine version using superconducting RF cavities. The aim there is to demonstrate that we are indeed dealing with a gauge theory. Processes of particular interest are the production of Higgs' particles, the study of the $Z^0 \rightarrow W^+W^-$ vertex, etc.

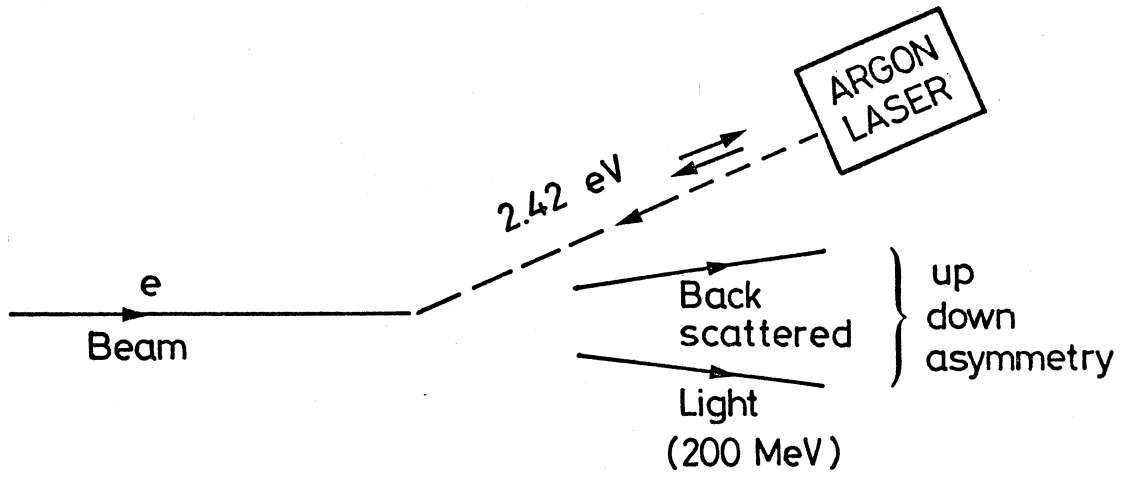


Figure 9 : Schematic arrangement of the SPEAR polarimeter (SLAC-Wisconsin)

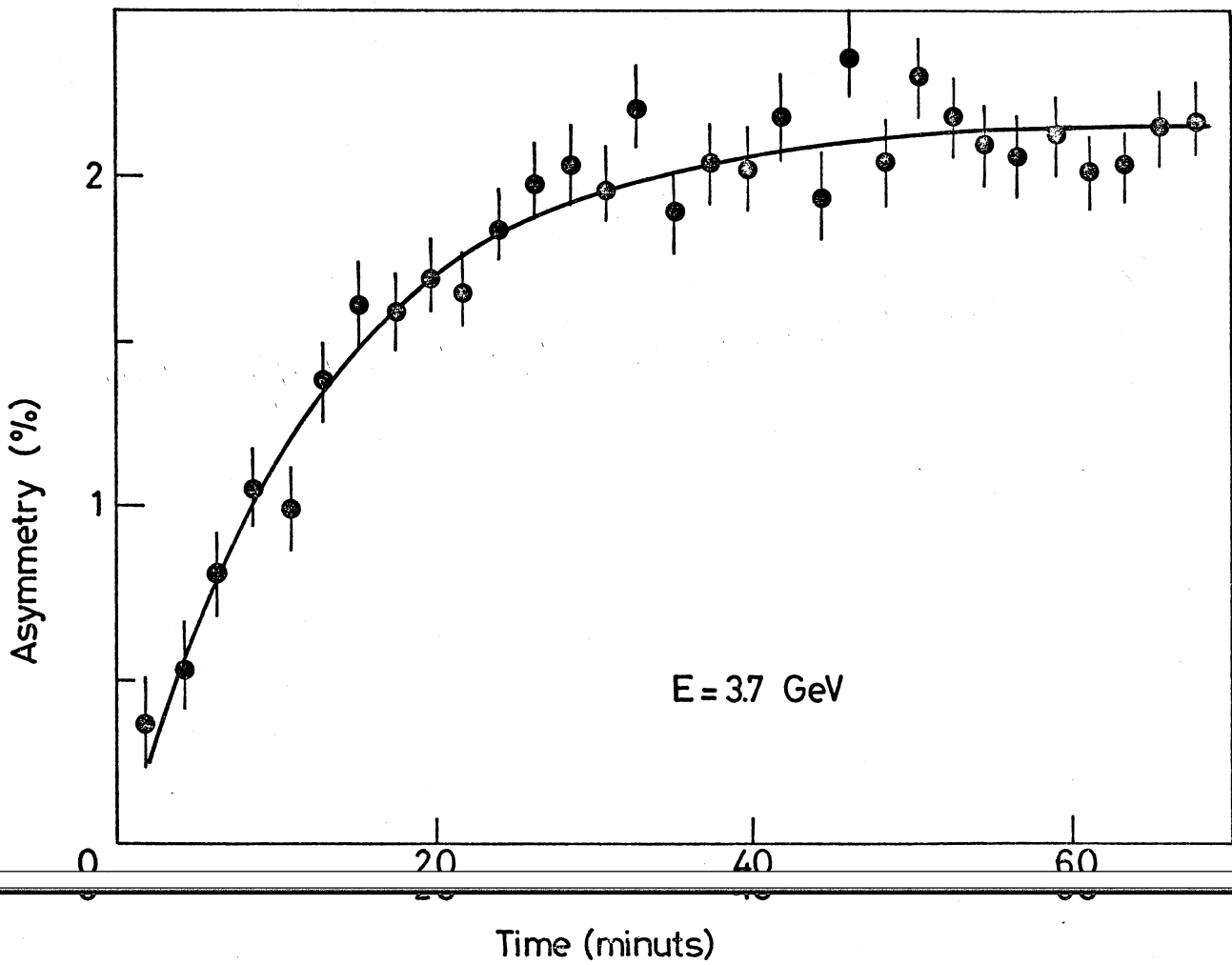


Figure 10 : Spontaneous build-up of transverse polarization at SPEAR

Single e^+ beam

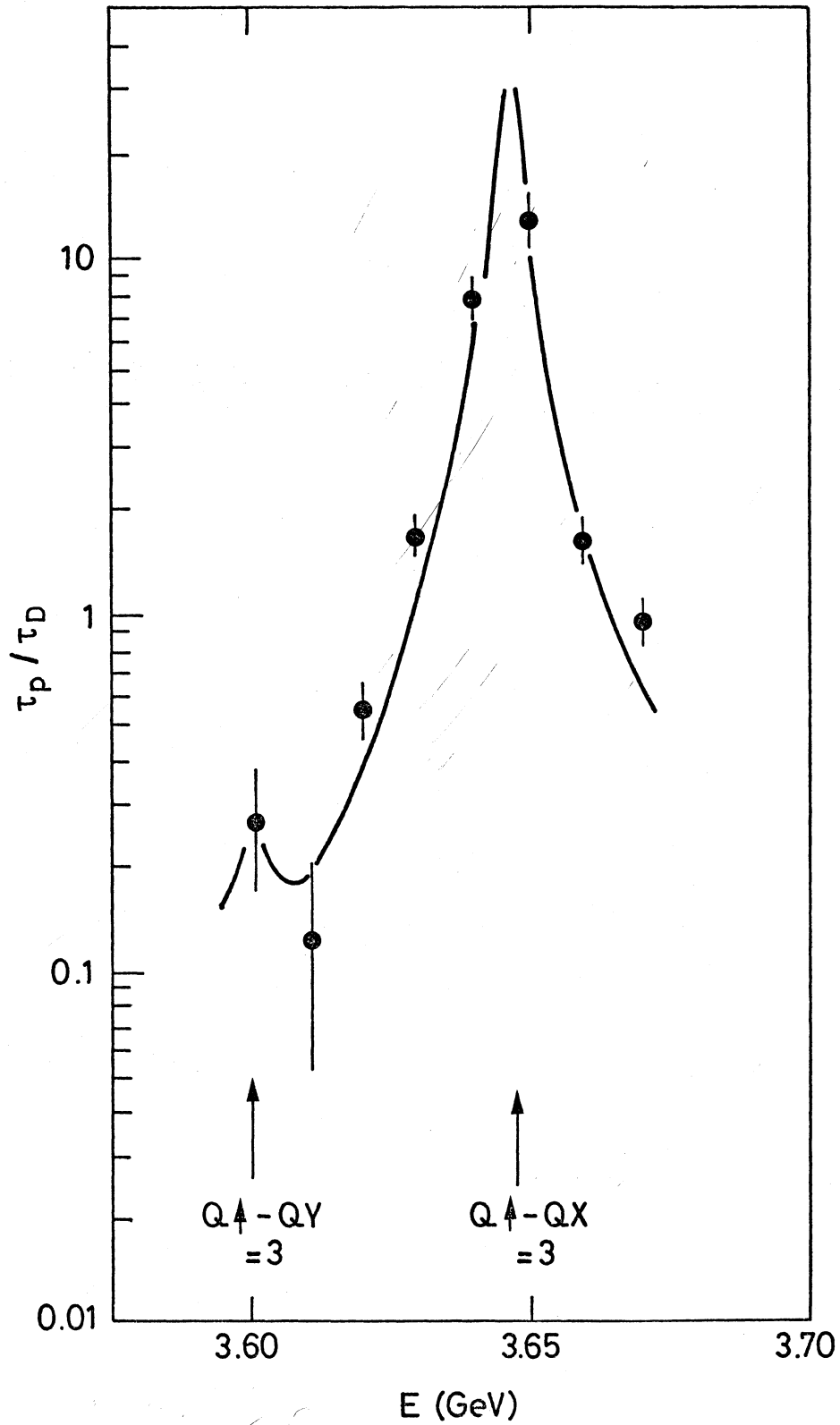


Figure 11 : The measured ratio τ_p / τ_D between the polarization and depolarization times as a function of energy. The full line is the result of a calculation accounting for depolarizing resonances

In each region individual reactions have been considered by the working groups¹⁾ and the importance of a polarized beam facility has been assessed for each of them separately. A general conclusion is that in the framework of theories containing only few parameters - such as SU(2) \times U(1) - polarization does not bring much additional information, a result which could be expected. But in all cases polarized beams appear to be very powerful revelators of unorthodox couplings. Rather than review a long list of different reactions, I shall instead illustrate the above statements by choosing two processes, typical of each of the two regions: annihilation processes proceeding via a Z^0 intermediate state and pair production of W^\pm bosons.

3.1 Annihilation Processes³⁾

The Z^0 coupling to a fermion-anti-fermion pair $\bar{f}f$ (Fig. 12) is given by

$$-M_Z \left[\frac{G_F}{\sqrt{2}} \right]^{\frac{1}{2}} \bar{f} \gamma_\mu \frac{v_f - a_f \gamma_5}{\sqrt{2}} f \quad (15)$$

where M_Z is the Z^0 mass, G_F the Fermi constant and v_f , a_f the vector and axial-vector couplings. The cross-section for $\bar{f}f$ production depends on the helicities of the incident electrons and outgoing fermions. In particular

$$\sigma (h_f = h_{\bar{f}} = \pm 1) = \sigma (h_e = h_{\bar{e}} = \pm 1) = 0 \quad (16)$$

More generally we may write

$$\frac{d\sigma}{d \cos \theta} = \frac{\alpha G_F M_Z^2}{16 \sqrt{2} (s - M_Z^2)} \left\{ f + h g \right\} \quad (17)$$

with two possible interpretations of Eq. 17:

- (i) the incident electrons are polarized, with helicities $h_e = h$, $h_{\bar{e}} = -h$ and no analysis is performed of the final state helicities;
- (ii) the incident beams are unpolarized but the final state helicities are analysed, $h_f = h$, $h_{\bar{f}} = -h$.

In both cases, a measurement of g is performed (f is simply obtained from the angular dependence of the cross-section measured with unpolarized beams). Explicit forms for g are:

- (i) $g = A (1 + \cos^2\theta) + 2 B \cos \theta$
- (ii) $g = B (1 + \cos^2\theta) + 2 A \cos \theta$

where A and B exchange each other when (a_e, v_e) and (a_f, v_f) are permuted.

$$\begin{aligned} A &= a_f (Q_f v_e - \chi v_f (a_e^2 + v_e^2)) \\ B &= a_e (Q_f v_f - \chi v_e (a_f^2 + v_f^2)) \end{aligned} \quad (19)$$

Here
$$\chi = \frac{G_F}{8\sqrt{2}\pi\alpha} \frac{s M_Z^2}{s - M_Z^2}$$

and Q_f is the charge of f . For $f\bar{f} = e\bar{e}$ we obtain $g \propto (1 + \cos\theta)^2$.

It therefore appears that measurements (i) and (ii) provide the same information in principle. However it should be noted:

- that (i) and (ii) suffer from very different systematic uncertainties: knowledge of the beam polarization, necessity to perform two different measurements in one case; knowledge of the analysis power, difficulty to deal with quark jets in the other;
- that (i) and (ii) have different angular dependences, the coefficient of $(1 + \cos^2\theta)$ in one case being that of $2 \cos\theta$ in the other and vice-versa.

The additional information provided by a measurement of g is only the sign of v/a . However, g has a better sensitivity to a small v contribution than a simple measurement of the angular dependence of the unpolarized cross-section. We also note that using polarized beams permits control over different quark flavours, or conversely, eases the experimental measurement of different quark flavour couplings. For example in $SU(2) \times U(1)$ with $\sin^2\theta_W = \frac{1}{4}$

$$\begin{aligned} a_e &= a_\mu = -1 & v_e &= v_\mu = 0 \\ a_u &= a_c = 1 & v_u &= v_c = 1/3 \\ a_d &= a_s = -1 & v_d &= v_s = -2/3 \end{aligned}$$

and

$$\begin{aligned} A_e &= A_\mu = 0 & B_e &= B_\mu = 0 \\ A_u &= A_c = \frac{\chi}{3} & B_u &= B_c = -\frac{2}{9} \\ A_d &= A_s = -\frac{2\chi}{3} & B_d &= B_s = -\frac{2}{9} \end{aligned}$$

How this fact can be exploited in practice is investigated in the summary report by K. Winter¹).

Therefore a polarized beam facility provides some convenience in the framework of a theory containing only point-like vector and axial couplings but is not at all essential. A radically different conclusion would be reached if nature would appear more complex than we now believe; in particular polarized beams provide a sensitive revelator of scalar couplings.

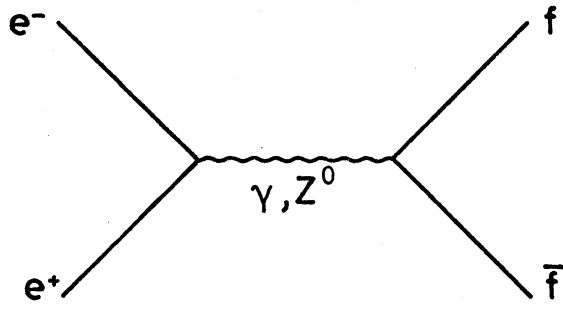


Figure 12 : Annihilation into a $f\bar{f}$ pair via a (Z^0, γ) intermediate state

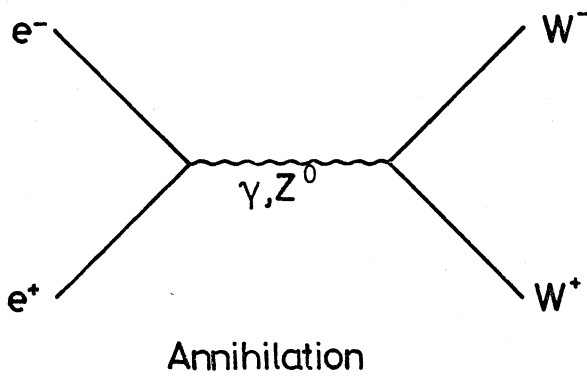
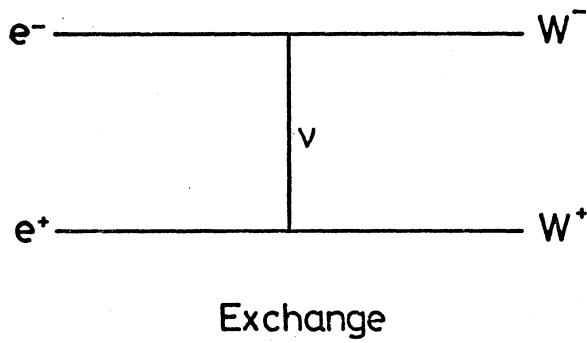


Figure 13 : The exchange and annihilation diagrams contributing to W^\pm pair production

3.2 Pair Production of W^\pm Bosons³⁾

Pair production of W^\pm bosons is expected to proceed via two different mechanisms (Fig. 13): a neutrino exchange diagram to which $e_L^- e_R^+$ contributes alone, and an annihilation diagram having both $e_L^- e_R^+$ and $e_R^- e_L^+$ contributions. Here again beams of equal helicities yield zero cross-sections. Cancellations between the different contributions are inherent to gauge theories and, as a result, $\sigma(e_R^- e_L^+) \ll \sigma(e_L^- e_R^+)$. To differentiate between various possible gauge theories would require a detailed study of the annihilation diagram, and imply disentangling the more trivial exchange diagram. A possible approach is to take advantage of the different angular distributions corresponding to the annihilation and exchange diagrams. However, because of the low expected event rate (≈ 2000 events for an integrated luminosity of 10^{38} cm^{-2}), the sensitivity of the method is not very satisfactory¹¹⁾. Another approach would be to switch off the exchange contribution by using polarized beams with helicities $e_R^- e_L^+$, but here again the expected rates are much too small (Fig. 14). Differentiating between various gauge theories from a study of the $Z^0 W^+ W^-$ vertex appears therefore to be a very difficult task. However, the mere observation of a strong decrease of the production rate when switching from $e_L^- e_R^+$ to $e_R^- e_L^+$ would provide an important evidence that we are indeed dealing with a gauge theory, or more precisely, its non-observation would be a good revelator of non-gauge theories.

Also, from a purely pragmatic point of view, event rates are multiplied by a factor of ≈ 4 when the incident beams are fully polarized in the $e_L^- e_R^+$ helicity state as compared to unpolarized beams. The importance of this enhancement should not be ignored: a large event rate in this channel will help the study of interference between the annihilation and exchange diagrams and possibly permit evidencing second-order effects.

3.3 Summary

In annihilation processes proceeding via point-like vector and axial-vector couplings polarized beams permit a measurement of the sign of v/a , a result which can be obtained as well from an analysis of the final-state helicities. However, they are sensitive revelators of other couplings.

The study of the $Z^0 W^+ W^-$ vertex, which is important in differentiating between various gauge theories, appears to be a difficult task, even when using polarized beams. However colliding different incident helicity states would be a powerful revelator of non-gauge theories.

In addition, a polarized beam facility would bring convenience for experimentation at LEP: possibility to perform cross-check measurements, to understand the 2γ background, to enhance annihilation rates, etc.

$\sqrt{s} = 200 \text{ GeV}$

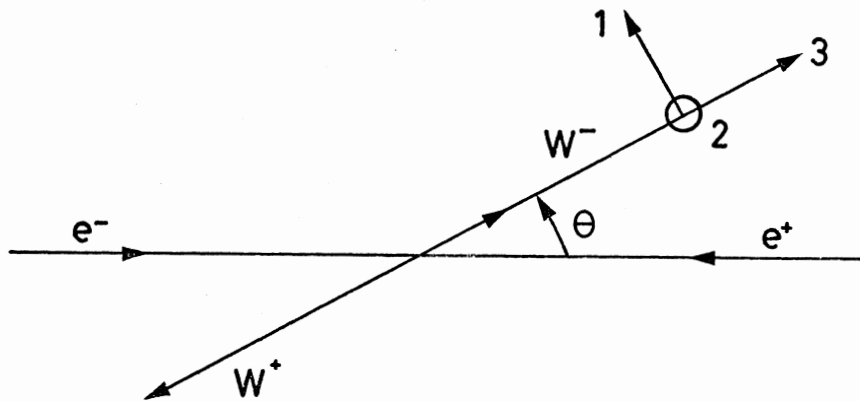
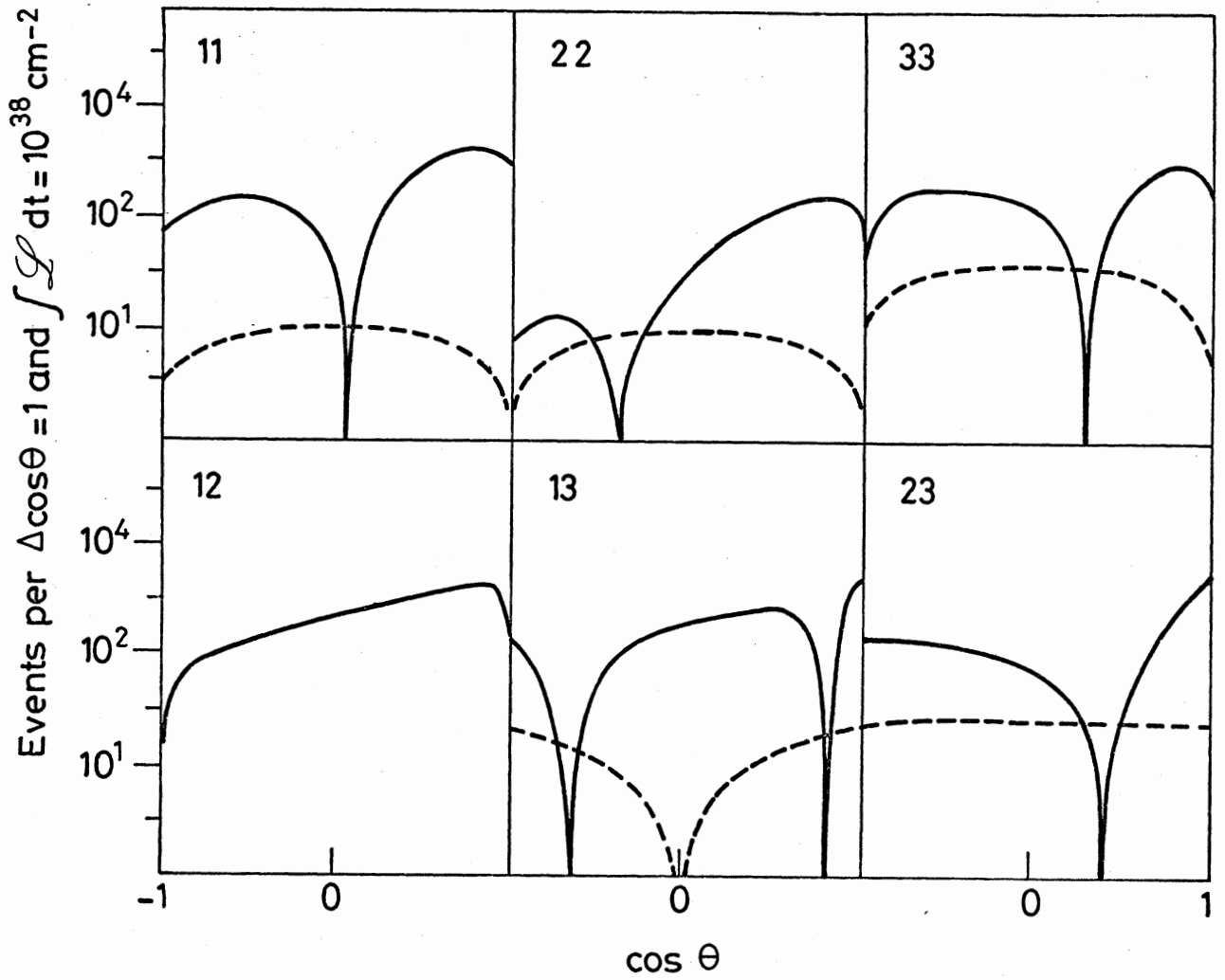


Figure 14 : Contributions to $W^+ W^-$ production from an $e^- e^+$ state (full line) and an $e^- e_L^+$ state (dotted line) for each of the final-state helicity configurations (axes 1, 2 and 3 are defined in the lower part of the figure). From K. Gaemers and G. Gounaris, reference 3

4. Conclusions

Having briefly assessed the benefits which a polarized beam facility would provide at LEP and being aware of the technical difficulties attached to its implementation, of the constraints it imposes on the machine design and of the limitations in its expected performance, we may conclude by drawing the following guide lines:

- (i) avoid taking any step which might preclude implementation of a polarized beam facility; such a facility may become a very useful revelator of unorthodox phenomena;
- (ii) within conventional gauge theories, and in particular if $SU(2) \times U(1)$ is sufficient to describe all aspects of weak and electromagnetic interactions, it is difficult to make a strong case for polarization; it seems therefore appropriate to keep it as an option to be implemented at a later stage;
- (iii) continued studies of possible depolarization effects and of alternatives to the Siberian Snake scheme should be actively pursued

* * * * *

Acknowledgements

I wish to express my gratitude to all my colleagues at Les Houches who helped in putting together the relevant arguments. I am especially indebted to B. Montague who introduced me to the subject and read carefully the manuscript and to R. Schwitters for illuminating comments.

References

1. See other Summary Reports in these Proceedings
2. B. Montague, LEP/70-10, LEP/70-76 and CERN/ISR-LEP/78-17; B. Montague and D. Möhl, CERN Yellow Report 76-18 and Nucl. Inst. & Meth. 137 (1976) 423
3. J. Ellis and M.K. Gaillard, CERN Yellow Report 76-18
K.J.F. Gaemers and G.J. Gounaris, CERN Report TH 2548-CERN, August 1978
4. A.A. Sokolov and I.M. Ternov, Sov. Phys. JETP 4(1957) 396, and
Sov. Phys. Doklady 8(1964) 1203
5. Ia. S. Derbenev, A.M. Kondratenko, et al., Particle Acc. 8 (1975) 115,
and Novosibirsk preprint I Ia F 76-84, 1976
6. V.N. Baier, Proceedings of the 46th Varenna Summer School on Electron Storage
Rings; J.D. Jackson, Rev. Mod. Phys. 48 (1976) 417
7. R. Schwitters, ECFA/LEP 40
8. O. Koffoed-Hansen (private communication) has pointed out that abundant
literature on field topologies similar to that of the snake is available
in fusion research
9. There exists a possibility of some spontaneous build-up of longitudinal
polarization when using the snake; see Ref. 5
10. R. Schwitters, Polarization measurements at SPEAR, presented at Les Houches
11. P. Darriulat and M.K. Gaillard, ECFA/LEP 1.